In-situ growth of superconducting NdFeAs(O,F) thin films by Molecular Beam Epitaxy

T. Kawaguchi[1,3*], H. Uemura[1,3], T. Ohno[1,3], M. Tabuchi[2,3], T. Ujihara[1,3],
K. Takenaka[1,3], Y. Takeda[1,3] and H. Ikuta[1,3]

[1]Department of Crystalline Materials Science, Nagoya University,
Chikusa-ku, Nagoya 464-8603, Japan
[2]Venture Business Laboratory (VBL), Nagoya University,
Chikusa-ku, Nagoya 464-8603, Japan
[3]JST, Transformative Research-Project on Iron Pnictides (TRIP),
Sanbancho 5, Chiyoda-ku, Tokyo 102-0075, Japan

May 4, 2010

The recently discovered high temperature superconductor F-doped LaFeAsO[1] and related compounds[2–10] represent a new class of superconductors with the highest transition temperature (T_c) apart from the cuprates. The studies ongoing worldwide are revealing that these Fe-based superconductors are forming a unique class of materials that are interesting from the viewpoint of applications. To exploit the high potential of the Fe-based superconductors for device applications, it is indispensable to establish a process that enables the growth of high quality thin films. Efforts of thin film preparation started soon after the discovery of Fe-based superconductors[11–13], but none of the earlier attempts had succeeded in an *in-situ* growth of a superconducting film of *Ln*FeAs(O,F) (*Ln*=lanthanide), which exhibits the highest T_c to date among the Fe-based superconductors. Here, we report on the successful growth of NdFeAs(O,F) thin films on GaAs substrates, which showed well-defined superconducting transitions up to 48 K without the need of an ex-situ heat treatment.

Thin film preparation of Co-doped AEFe$_2$As$_2$ (AE=Sr, Ba)[12,14–16] and iron-chalcogens[17–21] have been reported from many different research groups, the best films of which already possessing a T_c value exceeding 20 K. Quite recently, the fabrication of K-doped BaFe$_2$As$_2$ with an onset T_c up to 40 K was also reported[22]. In contrast, the growth of thin films of *Ln*FeAsO, the so-called 1111 family, which possesses T_c values up to 55 K, has been confronted with more difficulties.

Hiramatsu *et al*. prepared La-1111 films by pulsed-laser deposition (PLD) on oxide crystalline substrates[11]. They have succeeded in obtaining epitaxial films, but the films did not show a superconducting transition. Soon thereafter, another group reported the growth of F-doped La-1111 that exhibited a superconducting transition, which was also prepared by PLD on oxide substrates[13,23,24]. However, it was necessary to treat these films ex-situ at significantly high temperatures to form the 1111 phase. The necessity of such heat treatment places a considerable burden on the processing of superconducting devices, and the development of a procedure that does not require a subsequent high-temperature treatment is a necessary next step.

While the above mentioned two groups had employed PLD methods, we have succeeded in growing Nd-1111 thin films by molecular beam epitaxy (MBE) in a previous work[25]. The films were grown on GaAs substrates, which also differentiates our work from the other studies. GaAs was selected because of the good lattice matching and the similarity in the atomic coordination around As with *Ln*-1111. We also expect that various growth techniques established in studies on semiconductors can be applied when GaAs is used as substrates, such as strain control by an appropriate alloy buffer, and that novel devices may be realized by combining a superconductor with a semiconductor.

The growth condition for obtaining a single-phased film of Nd-1111 with a very high reproducibility was identified from a detailed study in our previous work[25]. However, the film did not show a superconducting transition and the resistivity increased at low temperature. Because that film was only 15 nm thick, we speculated that it might have some structural imperfections and studied the effect of increasing the film thickness. As a result, we succeeded in obtaining as-grown, superconducting thin films of F-doped Nd-1111. The highest onset temperature T_c^{onset} of these films is 48 K with a zero resistance temperature T_c^0 of 42 K. For the best of our knowledge, these are the first 1111-phase thin films that showed superconducting transitions without the need of an ex-situ heat treatment, and the T_c values are the highest among all thin films of the Fe-based superconductors reported so-far.

Figure 1a shows out-of-plane θ-2θ XRD patterns of the Nd-1111 films grown with various growth time t_g. The optimal growth condition of our previous study[25] was employed except for the substrate temperature, which was slightly lowered to 650°C in an attempt to reduce the impurities that were observed in films grown with long t_g (see below). Except for the growth time, all other parameters were identical for the films shown in Fig. 1a. As can be seen, the films grown for $t_g \leq 3$

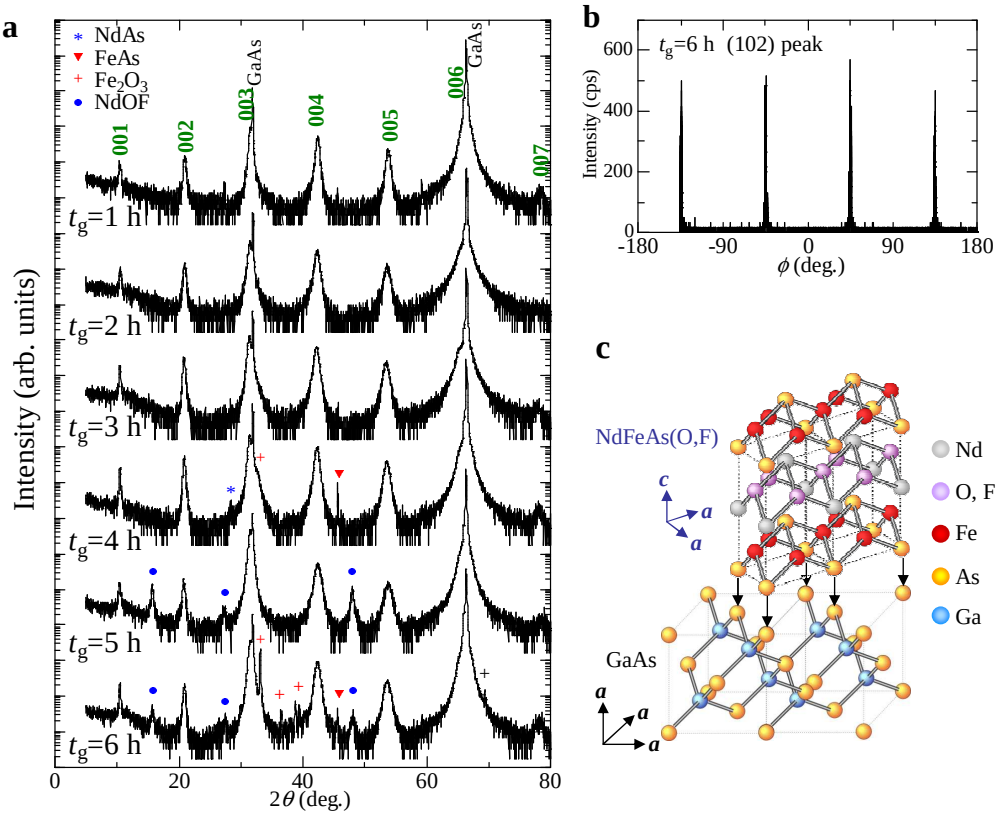

Figure 1: **X-ray characterization of the Nd-1111 films.** **a**, Out-of-plane θ-2θ XRD profiles of films grown with various growth times t_g. The growth parameters were identical for all films except the growth time. These profiles indicate that the Nd-1111 phase was grown with the *c*-axis perpendicular to the substrate in all films. **b**, Azimuthal phi-scan profile of the off-axis (102) reflection of the t_g=6 h film. A clear fourfold symmetry can be confirmed. **c**, A schematic drawing of the epitaxial relationship between the Nd-1111 phase and the GaAs substrate, which is consistent with the results of XRD analyses.

h were single-phased and all XRD peaks could be indexed as (00*l*) reflections from Nd-1111 except those arising from the substrate. With increasing the growth time further, however, the growth became somewhat unstable and some impurity peaks were observed in the XRD patterns. In particular, the formation of NdOF phase is obvious in the films grown for t_g=5 and 6 h. A fourfold symmetry was confirmed for the Nd-1111 phase in all films by measuring the azimuthal phi-scan of the (102) peak, as shown for example for the t_g=6 h film in Fig. 1b. These results indicate that the Nd-1111 phase was grown epitaxially on the substrate with the relation schematically shown in Fig. 1c.

Figure 2 shows the temperature dependence of resistivity ($\rho(T)$) of the Nd-1111 films. The film thickness that was necessary for converting resistance data to resistivity was calculated on the basis of the previously determined growth rate 15 nm/h (ref. 25), with the assumption that it did not depend on the growth time. As shown in Fig. 2a, the resistivity of the films grown for $t_g \leq 4$ h increased at low temperature similarly to the film we reported in our previous study[25] and did not show a superconducting transition. In a stark contrast, however, the t_g=5 and 6 h films shown in Fig. 2b exhibited a superconducting transition. T_c^{onset} and T_c^0 of the t_g=6 h film were slightly higher than the t_g=5 h film, and were 48 K and 42 K, respectively. The susceptibility of the t_g=6 h film, which is shown in the inset to Fig. 2b, confirms also a superconducting transition at about 40 K.

The difference between the $t_g \leq 4$ h and $t_g \geq 5$ h films can be attributed to F-contents. Figure 3 shows the temperature dependence of Hall coefficient of the Nd-1111 films. All films exhibited a negative Hall coefficient for the temperature range investigated. The magnitude of Hall coefficient of the $t_g \leq 4$ h films, which did not show a superconducting transition, increased steeply below about 200 K. On the other hand, the Hall coefficient of the t_g=5 and 6 h films had a much weaker temperature dependence. This change in the behavior of Hall coefficient corresponds quite well to the difference between non-doped and F-doped single crystals of Nd-1111[26], suggesting that the films grown for t_g=5 and 6 h were successfully doped with fluorine. Interestingly, the change in the behavior of Hall coefficient took place rather suddenly between t_g=4 and 5 h. The results of electron probe micro-analysis (EPMA) is consistent with this observation because no fluorine was found in the $t_g \leq 4$ h films while the t_g=5 and 6 h films contained a certain amount of fluorine.

Next, we would like to discuss why fluorine was observed only in the films that were grown with long t_g. Figure 4 shows the Auger depth profile of the t_g=6 h film, which is a plot of the intensity of the Auger signals as a function of the sputtering time t_{sp}. The interface between the

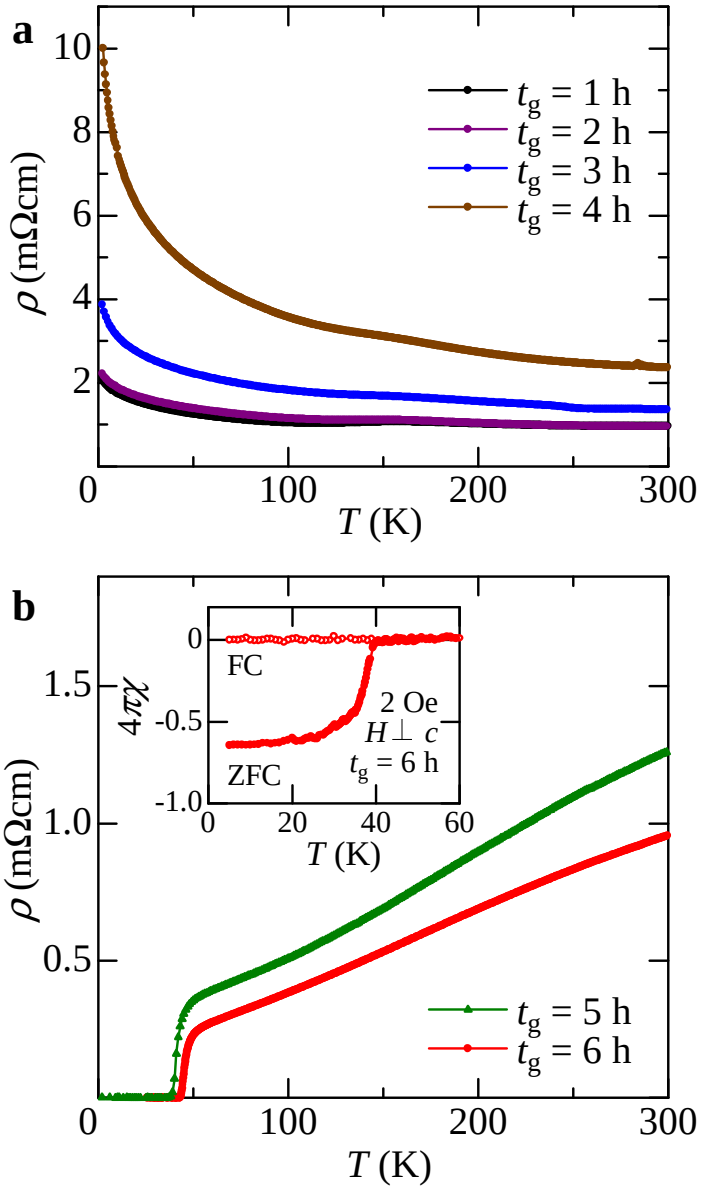

Figure 2: **Temperature dependence of resistivity of the Nd-1111 films.** **a**, $\rho(T)$ curves of the films grown for $t_g \leq 4$ h. **b**, $\rho(T)$ curves of the films grown for t_g=5 and 6 h. The films grown for $t_g \geq 5$ h exhibited clear superconducting transitions with $T_c^{\rm onset}$=45 K and T_c^0=38 K for the t_g=5 h film and $T_c^{\rm onset}$=48 K and T_c^0=42 K for the t_g=6 h film. The inset shows the temperature dependence of susceptibility of the t_g=6 h film.

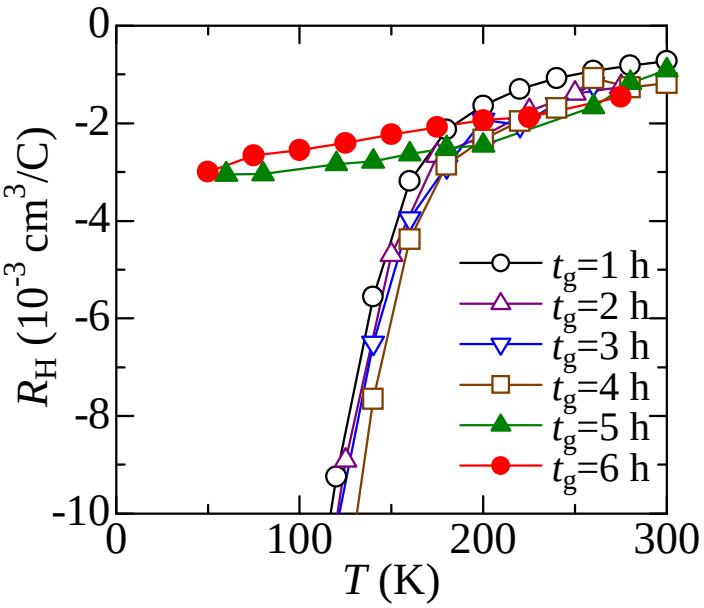

Figure 3: **Temperature dependence of Hall coefficient of the Nd-1111 films.** A rather sudden change in the behavior of Hall coefficient was observed between t_g=4 and 5 h, which corresponds quite well to the difference between the reported data of non-doped and F-doped bulk samples.

film and the substrate is evidenced by a rise in the Ga signal, and it can be seen that the contents of Nd, Fe, As, and O are nearly constant in the region above the interface for a certain range of thickness. The presence of fluorine was also confirmed, which is consistent with the conclusion of Hall coefficient and EPMA measurements. Very interestingly, however, we observed steep increases in Nd, O, and F contents near the surface ($t_{sp} \lesssim 200$ s) accompanied with depletion of Fe and As contents. This implies that the NdOF phase, that was observed in the XRD analyses of the t_g=5 and 6 h films, was formed at the end of the film growth. Indeed, the reflection high-energy electron diffraction (RHEED) pattern that was monitored during the growth suggested that the Nd-1111 phase was grown until $t_g \sim 4$ h, while a different phase, presumably NdOF, was dominant for $t_g \gtrsim 4$ h.

The change in the dominantly growing phase from Nd-1111 to NdOF at $t_g \simeq 4$ h was entirely unexpected for us because all processing parameters were kept to the same. However, we point out that the films were grown in an atmosphere that was probably quite excessive in fluorine. This is because NdF_3 was used as the source of Nd and F, which means that the supplied amount of F was three times larger than Nd. Therefore, what was unusual might be not the formation of NdOF but rather the Nd-1111 phase during the first stage of the film growth. It has been reported that fluorine can react with GaAs forming GaF_3 when GaAs is exposed to a F-containing vapor and the formed

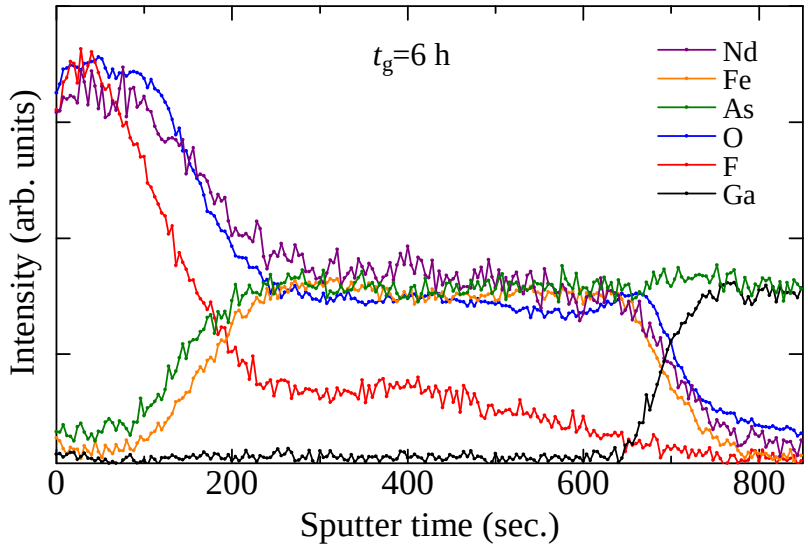

Figure 4: **Auger depth-profile analysis of the t_g=6 h Nd-1111 film.** The intensity of the Auger signal is plotted as a function of sputtering time. The purple, orange, green, blue, red, and black curves correspond to Nd, Fe, As, O, F, and Ga, respectively.

GaF_3 sublimates above about 550 K (about 280°C)[27,28]. We think that the same reaction took place at the early stage of the film growth, and the GaF_3 phase had immediately sublimated because the substrate temperature was 650°C. This consequently had an effect of regulating the amount of fluorine, and the Nd-1111 phase had grown. With the increase in the film thickness, however, reaching the GaAs surface became increasingly difficult for fluorine, and some of the fluorine remained unconsumed. When the amount of fluorine exceeded then a certain level, the growth of NdOF was thermodynamically more favorable, causing the change in the dominantly growing phase. SEM observations indicated that there exist some holes beneath the Nd-1111 films, which were absent when elemental Nd was used instead of NdF_3 as one of the sources. We think that these holes were formed due to the reaction of fluorine with the substrate, and support our growth model.

The present model can explain why the dominantly growing phase changed with the growth time. However, one would expect then that a F-doped Nd-1111 film with no NdOF should be obtained when the growth is stopped at $t_g \sim 4$ h. Nevertheless, the results of Hall coefficient and EPMA measurements indicate that this is not the case. A possible explanation for the lack of fluorine in the $t_g \leq 4$ h films is that fluorine may diffuse easily through Nd-1111 at high temperature and had escaped from the film after the supply of NdF_3 was stopped to terminate the growth. The NdOF phase that was grown in the $t_g \geq 5$ h films may have worked as a cap layer and had prevented

the loss of fluorine. In this respect, it is interesting that Kidszun *et al*. had mentioned that the formation of LaOF at the surface is a typical feature in their F-doped La-1111 films[24].

In summary, we have successfully grown superconducting films of Nd-1111. The as-grown films exhibited superconducting transitions when the growth time was sufficiently long with $T_c^{\rm onset}$ and T_c^0 up to 48 K and 42 K, respectively. While the films grown for $t_g \leq 3$ h were single-phased, we found a NdOF layer near the surface in the films that exhibited superconducting transitions. We think that this is because our films were grown in an excess supply of fluorine, but the presence of the cap layer may have played an important role to realize an as-grown superconducting film in the present work. This conclusion points some directions to which future studies should move to realize a film that is both single-phased *and* superconducting. First, it is preferable to avoid the reaction of fluorine with the substrate because it changes the amount of fluorine that contributes to the film formation and complicates the process. This may be achieved by using an appropriate buffer layer that protects GaAs. An independent control of Nd and F is also necessary because the excess supply of F seems to favor the formation of NdOF. Finally, the loss of fluorine from the film has to be prevented, which may be achieved by lowering the growth temperature. Studies in these directions are underway.

Methods

The thin films were grown by a MBE method, the detail of which is reported in the previous paper[25]. Briefly, GaAs(001) was used as substrates, on which an about 300-nm-thick GaAs buffer layer was grown at 610°C after the oxide layer on the substrate was removed by sublimation. Nd-1111 was grown by supplying all elements from solid sources charged in Knudsen cells; Fe, As, NdF_3, and Fe_2O_3. The substrate temperature was 650°C and the vapor pressures of Fe, As, NdF_3, and oxygen were 1.9×10^{-6}, 1.5×10^{-3}, 2.7×10^{-6}, and 2×10^{-5} Pa, respectively. The composition of the films was checked by electron probe micro-analysis (EPMA) using Nd-1111 powders as a reference. Depth-profile analysis was performed using an Auger electron spectroscopy (AES) combined with Ar ion sputtering (JEOL JAMP-7800). Scanning electron microscope (SEM) observation was performed using HITACHI S-4300. The growth rate of the films was estimated to be 15 nm/h in our previous study[25]. Resistivity was measured by a four-probe method, and susceptibility was measured using a SQUID magnetometer (Quantum Design MPMS-7). Hall coefficient was measured under a magnetic field of 9 T.

References

[1] Kamihara, Y., Watanabe, T., Hirano, M. & Hosono, H. Iron-Based Layered Superconductor La[$O_{1-x}F_x$]FeAs (x = 0.05–0.12) with T_c = 26 K. *J. Am. Chem. Soc.* **130**, 3296–3297 (2008).

[2] Chen, G. F. *et al.* Superconductivity at 41 K and Its Competition with Spin-Density-Wave Instability in Layered $CeO_{1-x}F_xFeAs$. *Phys. Rev. Lett.* **100**, 247002 (2008).

[3] Ren, Z.-A. *et al.* Superconductivity at 55 K in Iron-Based F-Doped Layered Quaternary Compound Sm[$O_{1-x}F_x$]FeAs. *Chin. Phys. Lett.* **25**, 2215 (2008).

[4] Ren, Z.-A. *et al.* Superconductivity and phase diagram in iron-based arsenic-oxides $ReFeAsO_{1-\delta}$; (Re = rare-earth metal) without fluorine doping. *Europhys. Lett.* **83**, 17002 (4pp) (2008).

[5] Kito, H., Eisaki, H. & Iyo, A. Superconductivity at 54 K in F-Free $NdFeAsO_{1-y}$. *J. Phys. Soc. Jpn.* **77**, 063707 (2008).

[6] Rotter, M., Tegel, M. & Johrendt, D. Superconductivity at 38 K in the Iron Arsenide $(Ba_{1-x}K_x)Fe_2As_2$. *Phys. Rev. Lett.* **101**, 107006 (2008).

[7] Tapp, J. H. *et al.* LiFeAs: An intrinsic FeAs-based superconductor with T_c = 18 K. *Phys. Rev. B* **78**, 060505 (2008).

[8] Hsu, F.-C. *et al.* Superconductivity in the PbO-type structure α-FeSe. *Proc. Natl Acad. Sci.* **105**, 14262–14264 (2008).

[9] Zhu, X. *et al.* Transition of stoichiometric Sr_2VO_3FeAs to a superconducting state at 37.2 K. *Phys. Rev. B* **79**, 220512 (2009).

[10] Sato, S. *et al.* Superconductivity in a new iron pnictide oxide $(Fe_2As_2)(Sr_4(Mg,Ti)_2O_6)$. *Supercond. Sci. Technol.* **23**, 045001 (2010).

[11] Hiramatsu, H., Katase, T., Kamiya, T., Hirano, M. & Hosono, H. Heteroepitaxial growth and optoelectronic properties of layered iron oxyarsenide, LaFeAsO. *Appl. Phys. Lett.* **93**, 162504 (2008).

[12] Hiramatsu, H., Katase, T., Kamiya, T., Hirano, M. & Hosono, H. Superconductivity in Epitaxial Thin Films of Co-Doped $SrFe_2As_2$ with Bilayered FeAs Structures and their Magnetic Anisotropy. *Appl. Phys. Express* **1**, 101702 (2008).

[13] Backen, E. *et al.* Growth and anisotropy of La(O,F)FeAs thin films deposited by pulsed laser deposition. *Supercond. Sci. Technol.* **21**, 122001 (2008).

[14] Katase, T. *et al.* Atomically-flat, chemically-stable, superconducting epitaxial thin film of iron-based superconductor, cobalt-doped $BaFe_2As_2$. *Solid State Commun.* **149**, 2121–2124 (2009).

[15] Iida, K. *et al.* Strong T_c dependence for strained epitaxial $Ba(Fe_{1-x}Co_x)_2As_2$ thin films. *Appl. Phys. Lett.* **95**, 192501 (2009).

[16] Lee, S. *et al.* Template engineering of Co-doped $BaFe_2As_2$ single-crystal thin films. *Nat. Mater.* **9**, 397–402 (2010).

[17] Han, Y. *et al.* Preparation and superconductivity of iron selenide thin films. *J. Phys.: Condens. Matter* **21**, 235702 (2009).

[18] Wang, M. J. *et al.* Crystal Orientation and Thickness Dependence of the Superconducting Transition Temperature of Tetragonal $FeSe_{1-x}$ Thin Films. *Phys. Rev. Lett.* **103**, 117002 (2009).

[19] Mele, P. *et al.* Fabrication of Fe–Te–S Superconducting Epitaxial Thin Films by Pulsed Laser Deposition. *Appl. Phys. Express* **2**, 073002 (2009).

[20] Bellingeri, E. *et al.* T_c=21 K in epitaxial $FeSe_{0.5}Te_{0.5}$ thin films with biaxial compressive strain. *Appl. Phys. Lett.* **96**, 102512 (2010).

[21] Imai, Y. *et al.* Systematic Comparison of Eight Substrates in the Growth of $FeSe_{0.5}Te_{0.5}$ Superconducting Thin Films. *Appl. Phys. Express* **3**, 043102 (2010).

[22] Lee, N. H., Jung, S.-G., Kim, D. H. & Kang, W. N. Potassium-doped $BaFe_2As_2$ superconducting thin films with a transition temperature of 40 K. *arXiv* 1004.4751v1 (2010).

[23] Haindl, S. *et al.* High Upper Critical Fields and Evidence of Weak-Link Behavior in Superconducting $LaFeAsO_{1-x}F_x$ Thin Films. *Phys. Rev. Lett.* **104**, 077001 (2010).

[24] Kidszun, M. *et al.* Epitaxial $LaFeAsO_{1-x}F_x$ thin films grown by pulsed laser deposition. *Supercond. Sci. Technol.* **23**, 022002 (2010).

[25] Kawaguchi, T. *et al.* Epitaxial Growth of NdFeAsO Thin Films by Molecular Beam Epitaxy. *Appl. Phys. Express* **2**, 093002 (2009).

[26] Cheng, P. *et al.* Hall effect and magnetoresistance in single crystals of $NdFeAsO_{1-x}F_x$ (x=0 and 0.18). *Phys. Rev. B* **78**, 134508 (2008).

[27] Freedman, A. & Stinespring, C. D. Halogenation of gallium arsenide(100) and (111) surfaces using atomic beams. *The Journal of Physical Chemistry* **96**, 2253–2258 (1992).

[28] Simpson, W. C., Durbin, T. D., Varekamp, P. R. & Yarmoff, J. A. The growth of GaF_3 films on GaAs(110) at elevated temperatures studied with soft x-ray photoelectron spectroscopy. *J. Appl. Phys.* **77**, 2751–2758 (1995).

Acknowledgement

This work was supported by Transformative Research Project on Iron Pnictides (TRIP), Japan Science and Technology Agency (JST).